

Calf Lung Surfactant Recovers Surface Functionality After Exposure to Aerosols Containing Polymeric Particles

Amir M. Farnoud, PhD,¹ and Jennifer Fiegel, PhD^{1,2}

Abstract

Background: Recent studies have shown that colloidal particles can disrupt the interfacial properties of lung surfactant and thus key functional abilities of lung surfactant. However, the mechanisms underlying the interactions between aerosols and surfactant films remain poorly understood, as our ability to expose films to particles via the aerosol route has been limited. The aim of this study was to develop a method to reproducibly apply aerosols with a quantifiable particle dose on lung surfactant films and investigate particle-induced changes to the interfacial properties of the surfactant under conditions that more closely mimic those *in vivo*.

Methods: Films of DPPC and Infasurf[®] were exposed to aerosols containing polystyrene particles generated using a Dry Powder Insufflator[™]. The dose of particles deposited on surfactant films was determined via light absorbance. The interfacial properties of the surfactant were studied using a Langmuir-Wilhelmy balance during surfactant compression to film collapse and cycles of surface compression and expansion at a fast cycling rate within a small surface area range.

Results: Exposure of surfactant films to aerosols led to reproducible dosing of particles on the films. In film collapse experiments, particle deposition led to slight changes in collapse surface pressure and surface area of both surfactants. However, longer interaction times between particles and Infasurf[®] films resulted in time-dependent inhibition of surfactant function. When limited to lung relevant surface pressures, particles reduced the maximum surface pressure that could be achieved. This inhibitory effect persisted for all compression-expansion cycles in DPPC, but normal surfactant behavior was restored in Infasurf[®] films after five cycles.

Conclusions: The observation that Infasurf[®] was able to quickly restore its function after exposure to aerosols under conditions that better mimicked those *in vivo* suggests that particle-induced surfactant inhibition is unlikely to occur *in vivo* due to an aerosol exposure.

Key words: aerosol, Infasurf, nanoparticles, surface tension, surfactant inhibition

Introduction

PULMONARY SURFACTANT IS A COMPLEX MIXTURE of lipids and proteins adsorbed at the air–water interface of the alveolar (gas exchange) region of the lungs. This surfactant layer reduces the surface tension of the alveolar fluid, thereby reducing the energy required to re-inflate the lungs. Pulmonary surfactant also reduces the surface tension of the alveolar fluid to near zero values, thereby maintaining the same recoil pressure in all alveolar sacs and avoiding alveolar collapse. Lung surfactant serves to maintain lung stability during normal respiratory maneuvers, and serious health implications can arise in the case of pulmonary surfactant

deficiency or dysfunction. Diseases such as respiratory distress syndrome and acute lung injury have been associated with pulmonary surfactant dysfunction.⁽¹⁾

Exogenous materials that interact with pulmonary surfactant have the capacity to deteriorate the surfactant's natural interfacial properties. Recent *in vitro* studies have reported alteration to the interfacial properties of lung surfactant after exposure to particles of both environmental and therapeutic relevance. Nano and submicron particle contaminants such as metal dust, TiO₂, biofuel combustion emissions, and silica have exhibited inhibitory effects on the interfacial properties of model pulmonary surfactants.^(2–7) Changes in surfactant phase behavior, minimum surface

Departments of ¹Chemical and Biochemical Engineering, and ²Pharmaceutical Sciences and Experimental Therapeutics, The University of Iowa, Iowa City, Iowa.

tension, and microstructure have also been observed after surfactant exposure to charged polymeric particles that are of particular interest in the field of aerosol medicine.^(8–13)

Surfactant function has been successfully studied using techniques that monitor changes in surfactant behavior during surface area compression and expansion. *In vivo* studies of surfactant function have been reported (see, for example, Im Hof et al.¹⁴), though such studies are limited both in number and the mechanistic information about particle–surfactant interactions that they can provide. Thus, researchers have generally relied on *in vitro* studies to improve basic understanding of the natural function of lung surfactant, how disease states contribute to lung surfactant dysfunction, and aid the clinical development of lung surfactant replacement therapies. Primary among the *in vitro* techniques are the Langmuir–Wilhelmy balance, the captive bubble tensiometer, and the pulsating bubble surfactometer. In the Langmuir–Wilhelmy balance method, surfactant molecules are spread on top of an aqueous subphase in a Langmuir trough and are compressed and expanded using a movable partition. A tensiometer provides real-time measurements of surface tension, while the movement of the barriers mimics surface area changes during respiration. The primary advantages of the Langmuir–Wilhelmy balance are that the system allows for studies of surfactant properties over a wide range of surface tension values and also at slower, quasi-static cycling speeds facilitating mechanistic studies (see Duncan and Larson⁽¹⁵⁾ for a review on such work). Instruments that better mimic the geometry of alveoli such as captive bubble tensiometer or pulsating bubble surfactometer have also been used to study lung surfactant function. Both of these instruments work on the basis of spreading surface-active material on the surface of an air bubble and relating the shape of the bubble to the surface tension at the air–water interface. These systems allow for fast surfactant cycling, which better mimics the fast compression and expansion of surfactant during breathing.

More recently, these techniques have been used to examine the interactions between aerosols and lung surfactant, particularly focusing on particle-induced surfactant dysfunction.^(3–6,10–13,16–21) While the studies conducted to date have led to valuable information on the mechanisms of particle-induced surfactant dysfunction generally, none of the methods used to introduce particles to the surfactant film accurately mimic exposure to particles following inhalation. Aerosols have different size and morphology compared to single particles. Changes in these physical properties have been shown to affect particle–cell interactions (e.g., certain sizes and certain shapes are internalized more efficiently by macrophages)^(22,23) and are also likely to affect particle interactions with the pulmonary surfactant. Although this has been recognized as a limitation to current knowledge of particle–lung surfactant interactions,⁽²⁰⁾ work in this area has been hindered due to the technical challenges of exposing surfactant films to aerosols, characterizing aerosol properties, and measuring the deposited particle dose.

In the present study, we describe a new method that was developed to apply aerosols onto surfactant films within a Langmuir trough with a reproducible, measurable dose. The Langmuir–Wilhelmy balance was chosen for these studies due to the ability to garner mechanistic understanding of surfactant function, as well as the ability to apply aerosols

directly onto the surfactant surface, which cannot be achieved with the captive bubble tensiometer or pulsating bubble surfactometer systems due to their enclosed configuration. The effects of aerosols on the interfacial behavior of two surfactant systems were investigated: dipalmitoyl phosphatidylcholine (DPPC), the most abundant lipid component of human lung surfactant responsible for surface tension lowering, and lung surfactant extracted from calves (Infasurf[®]), a more complex system whose composition closely mimics that of native human surfactant. The interfacial properties of surfactant films after exposure to aerosols containing polymeric particles were examined via surface tensiometric studies.

Materials and Methods

Commercial reagents

R-DPPC was purchased from Genzyme Pharmaceuticals (Cambridge, MA) and used without further purification. Infasurf[®] is a commercially available clinical pulmonary surfactant and was a generous gift from ONY Inc. (Amherst, NY). Sodium chloride, calcium chloride, and HPLC-grade chloroform were purchased from Sigma-Aldrich (St. Louis, MO). Methanol was 99.9% pure and purchased from Research Product International (Mount Prospect, IL). All water used in experiments was obtained from a Barnstead NANOpure II system from Barnstead International (Dubuque, IA) and had a resistivity of 18.2 M Ω ·cm. Carboxyl modified polystyrene particles with a nominal size of 200 nm were purchased as suspensions from Invitrogen (Carlsbad, CA).

Particle characterization

Zeta potential and size distribution. Particles were characterized in a solution of 150 mM NaCl and 1.5 mM CaCl₂, which was adjusted to a pH of 7 using NaOH (henceforth referred to as the subphase solution). Particle size distribution was determined by dynamic light scattering (DLS), and zeta potential was determined by laser Doppler anemometry using a Zetasizer Nano ZS (Malvern Instruments, Worcestershire, UK). For these measurements, particles were diluted to approximately 0.01 g/L in the subphase solution, vortexed for 90 sec, and sonicated for 10 min by bath sonication three times. One mL of the suspension was loaded into clear disposable folded capillary cells (DTS 1060C cuvettes) for characterization. The nominal diameter of particles was verified using TEM. TEM samples were prepared by suspending washed and lyophilized particles in methanol. One drop of this suspension was placed on a Formvar and carbon coated 400 mesh copper TEM grid using a Pasteur pipette. Imaging was performed after the evaporation of methanol using a JEOL JEM-1230 (Peabody, MA) transmission electron microscope. Images were analyzed using the ImageJ software.²⁴ The diameters of at least 100 particles were measured to determine the average particle size.

The size distribution and morphology of particle aerosols were determined using a Hitachi 4800 Scanning Electron Microscope (SEM). For these experiments, double-sided black carbon tape was attached to a SEM stub. Aerosols were applied onto the carbon tape from the Dry Powder InsufflatorTM and then sputter coated with Au-Pt at 10 mA and at a pressure of 7×10^{-2} mBar for 3 min using an Emitech Sputter Coater K550 (Quorum Technologies, United Kingdom).

After imaging, the projected surface area of ~ 100 agglomerates were estimated using ImageJ software. Particle size was reported as the diameter of a sphere that has a projection area equal to that of the agglomerate, to enable comparison between the relative agglomerate size and individual particles. The frequency distribution of particles was determined by categorizing the estimated diameters in $0.1 \mu\text{m}$ bins and counting the number of particles in each bin. Particle counts in each bin were divided by the total number of counted particles to generate normalized particle frequency distributions. Particle cumulative distribution was generated by adding the normalized frequency in each bin with the normalized frequencies of all the previous bins and plotting them against particle diameter.

Surface area and chemical composition. Particle surface area was measured using the Brunauer, Emmett, Teller (BET) adsorption method. Approximately 100 mg of particles were washed and lyophilized for each experiment. Lyophilization was performed overnight using a Labconco FreeZone 4.5 liter freeze dry system (chamber pressure of less than 0.02 mbar and collector temperature of less than -50°C). Surface area was determined by nitrogen adsorption at 77.4 K using an automated surface area analyzer (Quantachrome BET Nova 4200e). The surface chemical composition of washed and lyophilized particles was determined using a Kratos XPS Ultra-Axis instrument under ultra high vacuum ($\sim 10^{-9}$ Torr). A monochromatic aluminum Al K α (1486.6 eV) was used to eject the electrons from the sample and a hemispherical sector analyzer was used to determine the kinetic energy of electrons. Survey scans were performed in the range of -5 eV to 1200 eV with a step size of 1 eV and high resolution scans were performed at regions of interest with a step size of 0.1 eV. CasaXPS software was used for XPS data analysis and spectra were calibrated using the carbon C 1s peak at 285 eV.

Surface pressure versus surface area isotherms

Tensiometric studies were conducted using a Langmuir-Willhelmy apparatus (Minitrough System 4, KSV Instruments Ltd., Finland). The trough was mounted on a stand placed in an enclosure to avoid contamination from airborne particles. The Langmuir trough apparatus consisted of a Teflon-coated trough and two hydrophilic Delrin barriers for symmetric compression. Delrin barriers were used in these studies because they have been shown to reduce monolayer leakage.²⁵ Surface pressure (the surface tension of pure subphase minus the surface tension in the presence of surfactant) was measured using a platinum Wilhelmy plate (perimeter = 39.24 mm, width = 19.62 mm, and height = 10 mm). The trough was filled with a freshly made subphase solution and was allowed to equilibrate to room temperature ($23.3 \pm 0.6^\circ\text{C}$) for 30 min, then aspirated to remove any surface impurities. Experiments were performed with two surfactants: DPPC and Infasurf[®]. DPPC monolayers were obtained by spreading 50 μL of a 1.22 g/L surfactant solution in chloroform using a Hamilton microsyringe. This amount of DPPC added to the surface led to an initial mean molecular area of 111.6 $\text{\AA}^2/\text{molecule}$. Infasurf[®] films were obtained by spreading 70 μL of a 1.22 g total phospholipids/L surfactant solution in chloroform/methanol (2/1 volume ratio) using a Hamilton syringe. This amount of Infasurf[®] led to an initial surface

pressure of 11.9 ± 0.6 mN/m allowing for the different phases of Infasurf[®] isotherm to be observed in one compression cycle. After addition of either surfactant solution to the interface and prior to surface tension experiments, the solvent was allowed to evaporate from the surface for 20 min.

Surface area modifications in the Langmuir trough were performed in two modes: film collapse studies and lung relevant experiments. Film collapse studies provide information on surfactant phase behavior, limiting mean molecular area and particle effects on surfactant collapse. Lung relevant experiments simulated surfactant cycling during respiratory cycles. In film collapse experiments, the surface area of the trough was compressed from the initial trough area of 558 cm^2 to 100 cm^2 (total surface area change of 458 cm^2) with a barrier speed of 10 mm/min ($1.5 \text{\AA}^2/\text{molecule} \cdot \text{min}$). For particle-surfactant interaction studies, a Dry Powder Insufflator[™] (model DP-4M for mouse, PennCentury, Wyndmoor, PA) was used to generate and apply aerosols containing washed and lyophilized polystyrene particles on the surface of the trough before the trough compression was initiated. For each experiment, the Insufflator was loaded with 4 mg of dry particles. A 3 mL disposable syringe was attached to the insufflator and the device was held 30 cm from of the surface of the trough (Fig. 1).

For aerosol generation, the plunger of the syringe was pushed three times manually to ensure complete discharging of the insufflator. To determine the effect of surfactant phase at the time of particle deposition on particle-surfactant interactions, aerosols were applied at the surfactant surface at surface pressures of 25 mN/m and 43 mN/m during compression. Finally, to determine the role of particle-surfactant interaction time on surfactant interfacial behavior, aerosol application at the surface was performed 3 or 6 hours before the start of surface compression, and then the surface area of the trough was compressed from the initial trough area of 558 cm^2 to 80 cm^2 with a barrier speed of 10 mm/min ($1.5 \text{\AA}^2/\text{molecule} \cdot \text{min}$). Control experiments for each interaction time were performed by puffing air (no particles) on surfactant surfaces at that time point.

Lung-relevant experiments were performed by compressing and expanding the surfactant films in the lung-relevant surface pressure range. This range was determined from graphs of surface tension versus lung volume obtained from excised animal lungs. Four published studies were used as reference.⁽²⁶⁻²⁹⁾ To estimate the lung volume and the corresponding surface tension during breathing cycles, a lung capacity of 6 L, a resting volume of 3 L, and a tidal volume (the volume of air entering the lungs in each breath) of 0.5 L were assumed.⁽³⁰⁾ Using these values, it was estimated that the lungs are compressed and expanded between 50% and 58% of total lung capacity in each normal breath. A surface tension range of 3–24 mN/m (surface pressure range of 69.7 mN/m to 48.7 mN/m at room temperature) was estimated as the lung-relevant surface tension range from the surface tension versus lung volume graphs. Lung-relevant experiments were performed by dynamic compression-expansion of the barriers for 10 cycles between the surface areas of 210 cm^2 and 185 cm^2 for DPPC films and 198 cm^2 and 124 cm^2 for Infasurf[®] films. The surface areas were chosen so that a lung-relevant surface pressure range was acquired in the first cycle. Fast compression and expansion was performed with a barrier speed of 150 mm/min (the

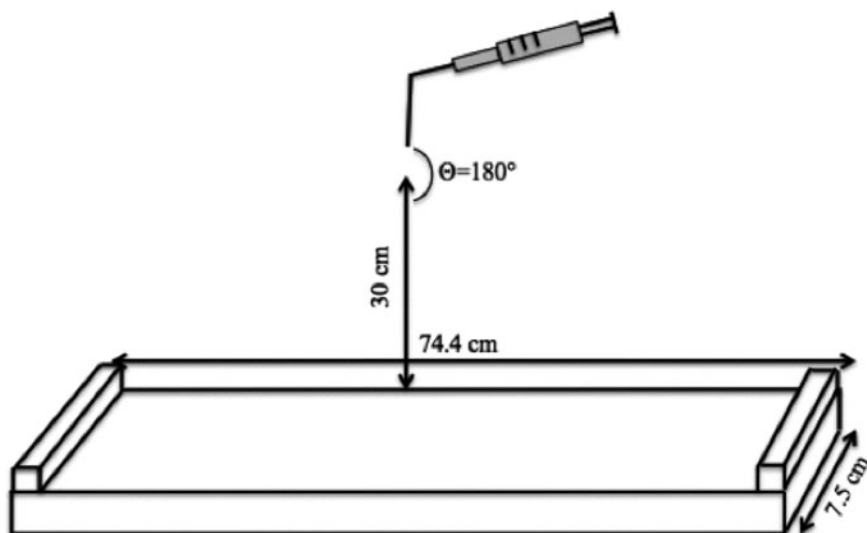


FIG. 1. Schematic of the experimental setup to achieve deposition of aerosols onto the surfactant surfaces. An insufflator was held vertically approximately 30 cm above the trough surface. A 3 mL syringe loaded with 200 nm carboxyl-modified polystyrene particles was attached to the insufflator, the plunger of the syringe was pushed three times manually to generate aerosols. The trough was equipped with a platinum Wilhelmy plate to measure the surface pressure (not shown).

highest barrier speed available on the instrument) to mimic the fast compression and expansion in the lungs. This resulted in a cycle time of 20 sec for DPPC and 43 sec for Infasurf[®] (due to the larger surface area compressions required to achieve the desired surface tensions). Cycling was performed in a square-wave manner with equal surface modification rates for both compression and expansion. Surface expansion was started immediately after the compression was completed. Particle-surfactant interaction studies in the lung-relevant surface pressure range were performed using the same barrier speed and surface area range. In these studies, aerosols were applied onto the surfactant films during the first expansion cycle. Control experiments were performed under similar conditions by puffing air (no particles) through the Dry Powder Insufflator[™] on the surfactant surface. All studies were performed at room temperature.

Particle dose quantification after deposition of aerosols on the surface

To obtain the concentration of particles deposited on the surfactant films, the content of the trough was analyzed by light absorbance. It has been previously shown that for small monodispersed particles, particle concentration has a linear relationship with absorbance.⁽²⁹⁾ A calibration curve of absorbance versus particle concentration was created for particle suspensions at concentrations of 7.5×10^{-4} g/L to 0.1 g/L. Prior to measurement of the calibration suspensions, they were vortexed for 90 sec and then sonicated for 10 min three times to ensure that particles were homogeneously suspended. The suspensions were then transferred to disposable polystyrene cuvettes (Sarstedt AG & Co., Germany) and their absorbance measured at a wavelength of 350 nm using a Spectramax Plus 384 Spectrophotometer (Molecular Devices, Sunnyvale, CA). For each sample, the absorbance was determined by subtracting the absorbance of the blank sample from the absorbance of the sample with particles. Samples that exhibited absorbance values of higher than 1 were diluted, since the Beer-Lambert law was no longer valid, and their obtained absorbance values were multiplied by the dilution factor.

To ensure the reproducibility of particle deposition, aerosols were applied onto the surface of two different troughs: the Langmuir trough (78.2 cm x 7.5 cm x 0.5 cm) and a custom made poly (methylmethacrylate) (PMMA) minitrough (7.5 cm x 12 cm x 0.6 cm). The subphase of the trough (volume of 250 mL for the Langmuir trough and 60 mL for the minitrough) was carefully transferred to a beaker using a pipette after the application of aerosols. Then the trough and the pipette were washed with a known volume of the subphase solution (50 mL for the Langmuir trough and 10 mL for the minitrough) to remove any remaining particles in the trough or inside the pipette leading to a known final volume (300 mL for the Langmuir trough and 70 mL for the minitrough). The beaker was sonicated in a bath sonicator for 15 min to ensure that the particles were dispersed homogeneously in the subphase. Then, the suspension in the beaker was transferred to test tubes and the test tubes were vortexed for 90 sec and sonicated for 10 min twice. The suspensions in the test tubes were transferred to disposable cuvettes and their absorbance at 350 nm was determined. Particle concentration in the subphase was determined from absorbance and multiplied by 6/5 for the Langmuir trough and by 7/6 for the minitrough to compensate for the additional volume added during trough cleaning. The average and standard deviation of particle concentrations after three experiments was reported in terms of g particles/L subphase.

Results

Particle characterization

Carboxyl-modified polystyrene particles with a nominal diameter of 200 nm were characterized to determine their surface area, surface functional groups, zeta potential, and size and size distribution in colloidal suspensions and as dry agglomerates. The mean diameter of the dried colloidal particles was 218 ± 18 nm as measured by TEM, and the hydrodynamic diameter of particles in colloidal suspension was 236 ± 5 nm as measured by DLS. The geometric size distribution of particles suspended in air using the insufflator was determined from SEM images (Fig. 2). About half of

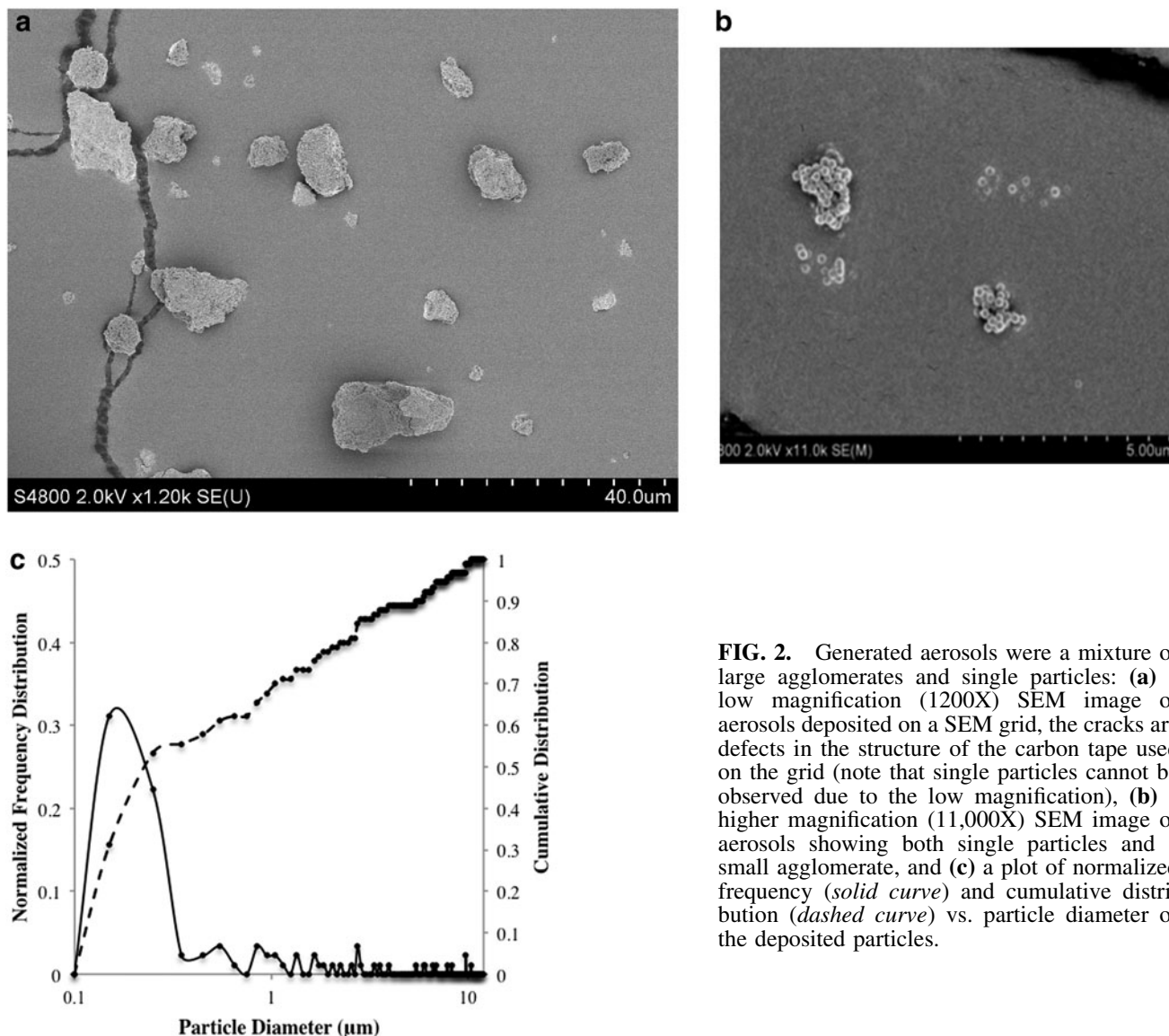


FIG. 2. Generated aerosols were a mixture of large agglomerates and single particles: (a) a low magnification (1200X) SEM image of aerosols deposited on a SEM grid, the cracks are defects in the structure of the carbon tape used on the grid (note that single particles cannot be observed due to the low magnification), (b) a higher magnification (11,000X) SEM image of aerosols showing both single particles and a small agglomerate, and (c) a plot of normalized frequency (*solid curve*) and cumulative distribution (*dashed curve*) vs. particle diameter of the deposited particles.

the particles (53%) exhibited a diameter of $0.3 \mu\text{m}$ or less, suggesting the presence of a large quantity of single particles after aerosol generation. However, agglomerates were also observed. The diameters of agglomerates (calculated from the projected surface area assuming spherical agglomerates) were within the range of $0.4 \mu\text{m}$ to $10.4 \mu\text{m}$. Although not all agglomerates were spherical (ellipsoidal and irregularly shaped agglomerates were observed in similar numbers), this assumption was used because it would allow for estimation of a diameter; thus, enabling a comparison between the sizes of single particles vs. agglomerates.

The cumulative particle distribution reached 100% at $10.4 \mu\text{m}$, confirming that all particles had an estimated diameter of $10.4 \mu\text{m}$ or less. Particles were negatively charged, with a zeta potential of $-28.4 \pm 2.9 \text{ mV}$ in the subphase solution. The surface area of the particles was measured to be $27 \pm 3 \text{ m}^2/\text{g}$ via the BET adsorption method. This value is very close to theoretical size of spherical particles with a diameter of 200 nm ($28.9 \text{ m}^2/\text{g}$), implying that particle surfaces were smooth and there was little or no aggregation. XPS analysis confirmed the

presence of 5.45% carboxyl group at the particle surface the carboxyl group with a peak at 289.48 eV .

Particle dose quantification after aerosol application on the surface

A major challenge in studying the effects of aerosols on lung surfactant function is estimating the dose of deposited particles. Although the initial and final weights of the insufflator were recorded and used to determine the amount of particle suspended in air, the concentration of particles actually depositing on the surfactant surface was lower due to particle loss to the walls of the Langmuir trough enclosure. Therefore, a method based on light absorbance was used to measure the amount of particles deposited on surfactant monolayers in the Langmuir trough. The light absorbance of the particle-laden subphase exhibited a linear relationship with particle concentration at a laser wavelength of 350 nm over a range of particle concentrations from $7.5 \times 10^{-4} \text{ g/L}$ to $1.0 \times 10^{-1} \text{ g/L}$ (Fig. 3). This observation was in agreement

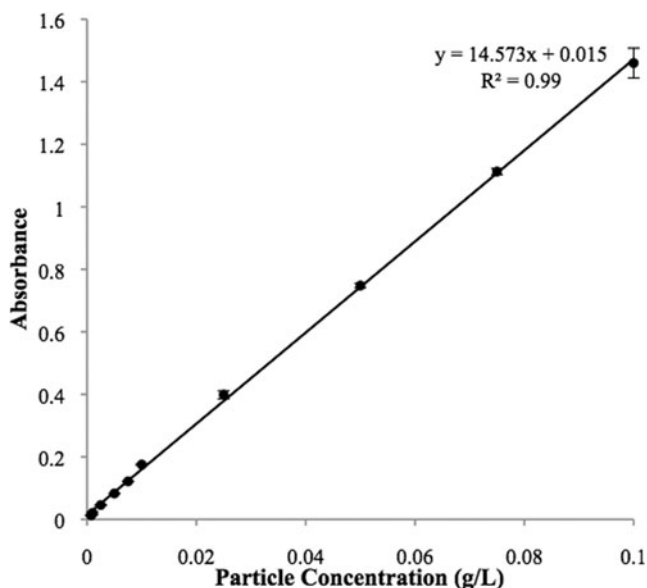


FIG. 3. Particle concentration vs. absorbance measured at a laser wavelength of 350 nm exhibited a linear correlation at concentrations from 7.5×10^{-4} g/L to 0.1 g/L. Absorbance of all particle suspensions was measured following vortex and sonication of the particle suspension.

with the report of Irache et al.,⁽³¹⁾ who used light absorbance at various wavelengths to measure particle concentrations.

In the current study, we aimed to achieve a deposited dose of 0.04 g/m^2 of particles, which corresponds to 5.7×10^{11} particles/ m^2 . This particle concentration overlaps with that from our previous studies using traditional routes of exposure (subphase injection of particles beneath a surfactant film or monolayer addition on a particle-laden subphase), enabling us to identify specific effects due to exposure to aerosols.^(11,12) Based on human particle exposure in pulmonary drug delivery applications or due to occupational exposures over the course of a day, we estimate that this deposited dose is about an order or magnitude larger than a physiologically relevant dose.⁽³²⁾ Interestingly, this concentration is significantly lower than that used in most literature studies where particle concentrations can be as high as 41 g/m^2 .⁽³²⁾

In the current study, dose reproducibility was verified by applying aerosols onto an aqueous surface within either a custom-made minitrough or the Langmuir trough used for tensiometric experiments. An initial powder amount of 3 mg was used for insufflation on the minitrough (surface area of 90 cm^2 and subphase volume of 60 mL). Particle insufflation led to the deposition of $1.79 \pm 0.34 \text{ mg}$ of particles in the minitrough ($n=11$). This amount of delivered particle was equal to $60 \pm 11\%$ of the particles initially loaded in the insufflator. In experiments with the Langmuir trough (surface area of 558 cm^2 and subphase volume of 250 mL), the insufflator was filled with 4 mg of particles, which were then suspended in air and deposited on the trough surface. Applying aerosols on this trough led to an average dose of $2.91 \pm 0.60 \text{ mg}$ ($n=25$). The amount of delivered particle in this case was equal to $71 \pm 14\%$ of the particles initially loaded in the insufflator and was not statistically different from the percentage of the delivered particles using the small trough.

Surface pressure isotherms-film collapse studies

Tensiometric studies were performed to examine the effects of particle exposure on the surface-active behavior of surfactant films. Effects were characterized by examining changes to the surface pressure (i.e., the difference between the surface tension of pure subphase and the surface tension in the presence of surfactant), surfactant phase behavior, and the maximum surface pressure (lowest surface tension) achievable. Initially, surfactant films were slowly compressed from a surface pressure of zero until a plateau in the maximum surface pressure was recorded, which corresponded to film collapse. These studies provided basic mechanistic information on the function of surfactant films in the presence and absence of particles.

Pure DPPC monolayers exhibited typical phase behavior upon surface compression (Fig. 4a, solid line). At large surface areas (above 500 cm^2), the gas phase was observed where the DPPC molecules do not interact with each other, resulting in no significant change in the surface pressure. Compression to smaller surface areas led to the development of the liquid expanded (LE) phase (between 500 cm^2 and 400 cm^2). In this phase, DPPC molecules begin to interact, resulting in an almost linear increase in the surface pressure. In this phase, the aliphatic tails of the phospholipid remain randomly oriented. Further compression of DPPC molecules resulted in the appearance of the liquid expanded-liquid condensed (LE-LC) phase (observed between 400 cm^2 and 300 cm^2). In this phase, patches of closely packed DPPC molecules with vertically oriented aliphatic tails are observed between liquid expanded phases as shown previously by fluorescent and atomic force microscopy.^(5,11,32) Reduction of the surface area to less than 300 cm^2 resulted in a transition to the liquid condensed (LC) phase where an exponential increase in surface pressure isotherm was observed. This phase was followed by a plateau in surface pressure at a value of $72.3 \pm 0.1 \text{ mN/m}$. This plateau denoted a transition from a single monolayer at the surface to multilayer formation, commonly known as monolayer collapse.³³ The surface pressure isotherm of DPPC on pure subphase solution and the onset of different phases were in agreement with previous reports.^(11,34)

Polystyrene particles were suspended in air and applied onto the DPPC films via a Dry Powder InsufflatorTM. Three independent experiments led to a deposited particle dose of $3.37 \pm 0.39 \text{ mg}$ ($0.060 \pm 0.007 \text{ g/m}^2$). At this concentration, particles showed little effect on the phase behavior of DPPC monolayers into the LC region (Fig. 4a, dashed line). Towards the end of the LC region (surface pressure of $\sim 60 \text{ mN/m}$), the presence of particles caused a slight reduction in the rate of surface pressure increase. This effect led to a shift in the surface area of monolayer collapse, which occurred at an average surface area of $162 \pm 3 \text{ cm}^2$ in the presence of particles compared to $174 \pm 3 \text{ cm}^2$ for pure DPPC monolayers. Exposure to particles did not induce a significant effect on the maximum surface pressure achievable by the DPPC monolayers ($72.2 \pm 0.8 \text{ mN/m}$ vs. $72.3 \pm 0.1 \text{ mN/m}$ for the monolayer without particles). Small changes in particle dose (in the range of 0.054 g/m^2 to 0.067 g/m^2) did not significantly alter the observed effects on the surface pressure isotherms (Fig. 4b).

To evaluate particle effects on a more complex lung surfactant system, experiments were conducted with Infasurf[®],

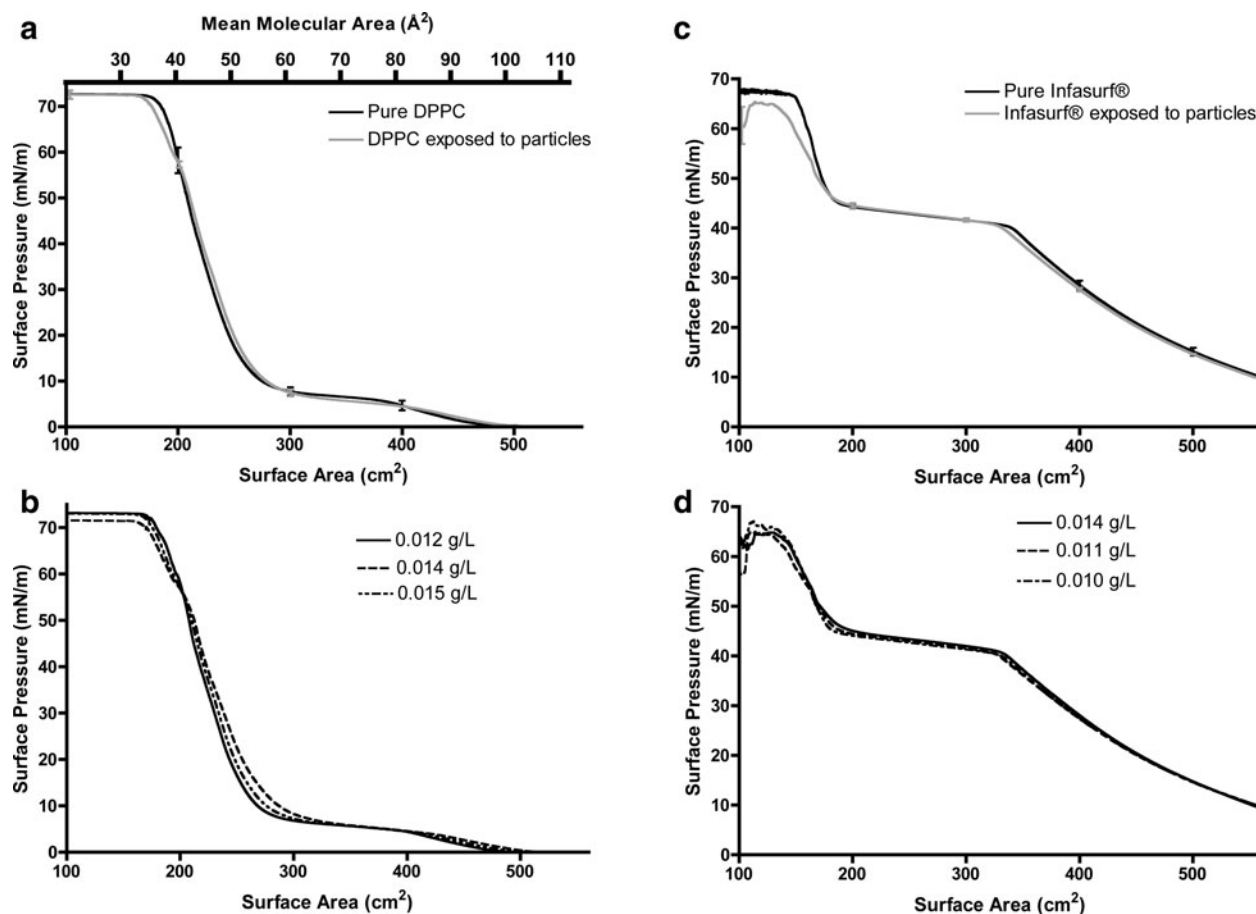


FIG. 4. Surface pressure vs. surface area isotherms of (a) DPPC films with no particles (*solid line*) and after exposure to aerosols (*dashed line*), (b) an overlay of three independent particle deposition experiments with exposure of DPPC films to particle concentrations ranging from 0.054 to 0.067 g/m², (c) Infasurf[®] films with no particles (*solid line*) and after exposure to aerosols (*dashed line*), and (d) an overlay of three independent particle deposition experiments with exposure of Infasurf[®] films to particle concentrations ranging from 0.045 to 0.063 g/m². Surface pressure isotherms were obtained by surface compression from an initial surface area of 558 cm² (111.5 Å²/molecule) to 100 cm² (20 Å²/molecule), which was initiated immediately after aerosol deposition. *Error bars* represent the standard deviation.

a calf lung surfactant extract used in surfactant replacement therapy.⁽³⁵⁾ Similar to pure DPPC monolayers, Infasurf films show distinct surface pressure regimes during lateral compression (Fig. 4c, *solid line*). However, it is important to note that the composition of these regimes are quite different from those observed for DPPC films. At surface pressures of less than 40 mN/m, surface compression resulted in an almost linear increase in surface pressure. In this region, three phases can be detected: a liquid-expanded, a tilted-condensed, and a cholesterol mediated liquid-ordered phase.⁽³⁶⁾ Starting from a surface pressure of 40.6 ± 0.3 mN/m a plateau in surface pressure was observed that continued to approximately 50 mN/m. Atomic force microscopy studies have shown that the liquid-expanded and liquid-ordered phases collapse during this plateau and the Infasurf film changes from a monolayer to a multilayer.^(10,36) At surface pressures above 50 mN/m, an exponential increase in the surface pressure was observed, which was followed by a plateau at a surface pressure of ~67 mN/m marking complete surfactant collapse. The shape of the Infasurf surface pressure isotherm and the surface pressure regimes observed in this study were in agreement with previously published reports.^(10,36)

Exposure to particles induced no significant change in the Infasurf[®] surface pressure isotherm at low surface pressure values. However, at surface pressures above 50 mN/m, a reduction in the rate of surface pressure increase was observed (Fig. 4c, *dashed line*). Similar to DPPC, a shift in the surface area of surfactant collapse was observed (149.2 ± 4.2 cm² for pure Infasurf vs. 129.0 ± 2.0 cm² in the presence of particles). In addition, Infasurf[®] films also experienced a reduction in the maximum surface pressure after exposure to particles (65.6 ± 1.3 mN/m vs. 68.3 ± 0.3 mN/m for pure Infasurf[®]), suggesting a different mechanism of inhibition compared to the DPPC films. An overlay of the three independent experiments with a deposited particle dose ranging from 0.045 g/m² to 0.063 g/m² (Fig. 4d) confirmed that small changes in particle concentration did not alter the observed Infasurf[®] behavior.

Surface pressure isotherms—Aerosol application at different stages of compression

Atomic force microscopy studies have demonstrated morphological changes of Infasurf[®] films during surface compression.^(36,37) Since it has been observed that Infasurf[®]

films transform from a monolayer to a multilayer during the surface pressure range of 40 mN/m to 50 mN/m,^(36,37) we were interested in the effects of aerosols onto surfactant films in these different phases. To this aim, aerosols were applied onto the surfactant film during surface compression of Infasurf[®] at surface pressures of 25 mN/m (surfactant as a monolayer) and 43 mN/m (within the monolayer-multilayer transition region). The dose of particles delivered to the films was similar to film collapse studies with a delivered dose of $0.045 \pm 0.004 \text{ g/m}^2$. In contrast to film collapse studies, exposure to aerosols during surface compression did not cause an inhibitory effect on the surface pressure isotherm of Infasurf[®] (Fig. 5a and 5b). At the point of aerosol deposition, a dip was observed in the surface pressure isotherm. However, the surfactant film quickly recovered and no further effects on the surface pressure isotherm could be observed. Neither the maximum surface pressure nor the

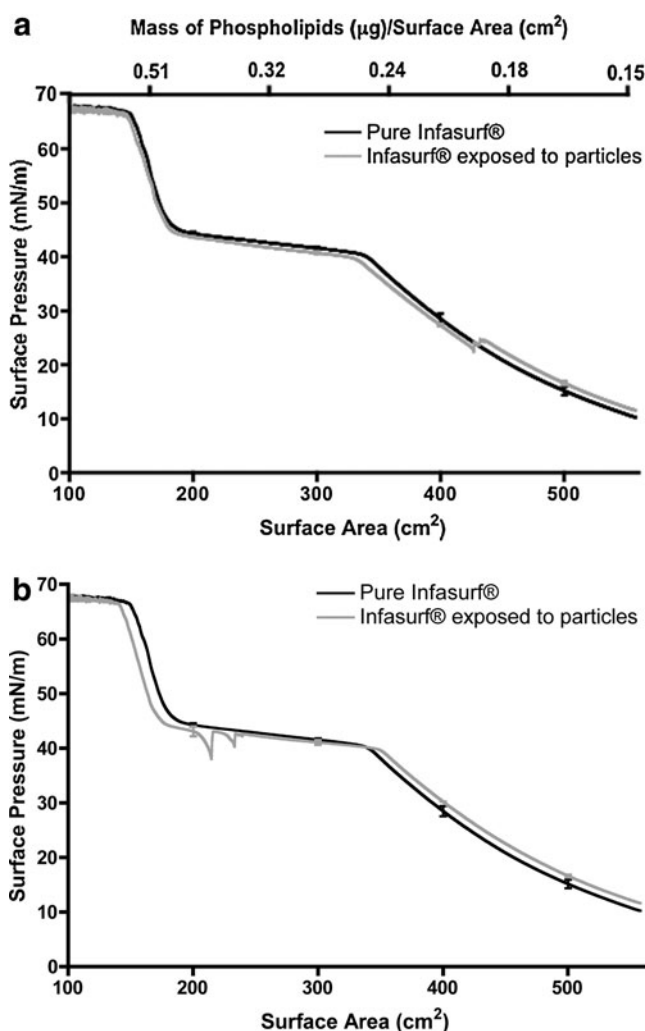


FIG. 5. Surface pressure vs. surface area isotherms of pure Infasurf[®] films (**bold line**) and Infasurf[®] films after deposition of particles at a surface pressure of (a) 25 mN/m and (b) 43 mN/m (*dashed lines*). Dips in the isotherm occur at the point of deposition. The surfactant films were compressed from an initial surface area of 558 cm² to 100 cm² ($0.15 \mu\text{g}$ to $0.85 \mu\text{g}$ of phospholipids per cm² of surface area). *Error bars* represent the standard deviation.

surface area of surfactant collapse were affected by particle deposition at either surface pressure.

Surface pressure isotherms—Adsorption time studies

The effects of small particles on the surface pressure isotherms of surfactant films are time-dependent.⁽¹⁰⁾ Thus, we studied the effects of interaction time on surfactant function by allowing the deposited particles to interact with the surfactant for 3 or 6 hours before starting the surface compression (Fig. 6). Longer interaction times resulted in a shift in the surface area of surfactant collapse and a reduction in the maximum surface pressure of Infasurf[®] films. These effects were observed after both 3 (Fig. 6a) and 6 hours (Fig. 6b) of interaction time.

Surface pressure isotherms—Lung relevant studies

To gain a better understanding of surfactant function under typical breathing conditions, we monitored surface pressure during 10 compression and expansion cycles under small surface area changes (25 cm²) cycling at a high rate of 150 mm/min ($22.5 \text{ \AA}^2/\text{molecule} \cdot \text{min}$ or $113 \text{ cm}^2/\text{min}$). This surface compression speed was 15 times faster than the speed used for film collapse studies, facilitating our understanding of

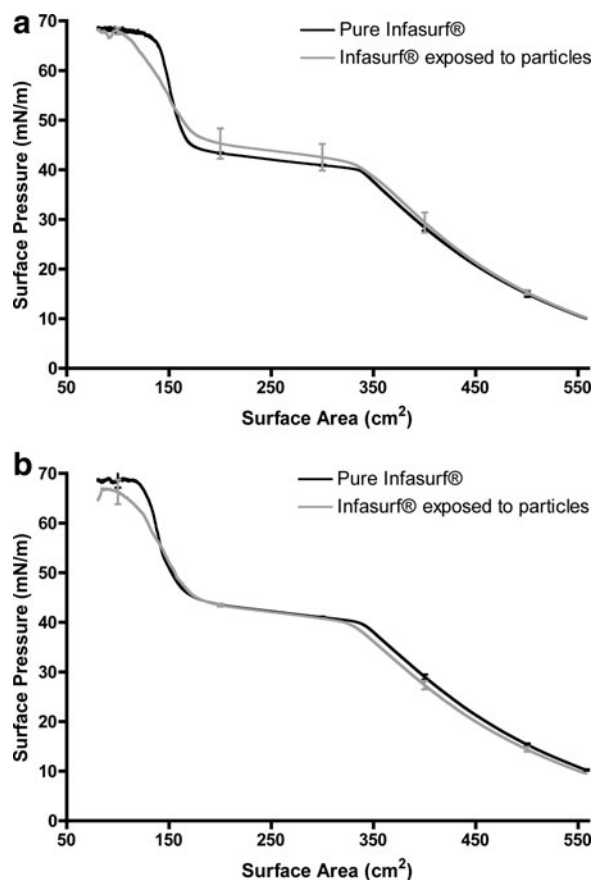


FIG. 6. Surface pressure vs. surface area isotherms of pure Infasurf[®] film (**bold line**) and Infasurf[®] film after (a) 3 hours of interaction and (b) 6 hours of interaction with deposited particles (*dashed lines*). The surfactant films were compressed from an initial surface area of 558 cm² to 100 cm². *Error bars* represent the standard deviation.

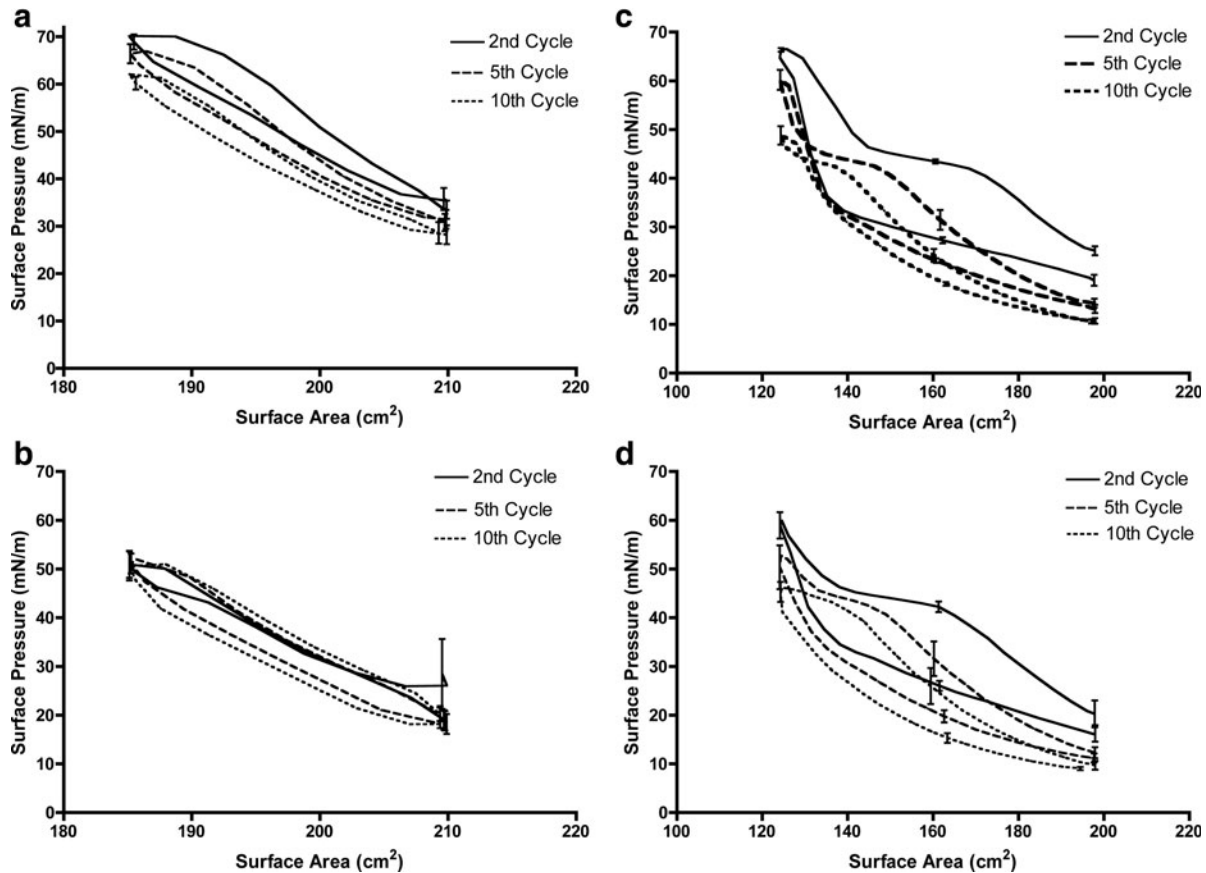


FIG. 7. Surface pressure vs. surface area isotherms of (a) pure DPPC monolayers, (b) DPPC monolayers after exposure to particles, (c) pure Infasurf[®] films, and (d) Infasurf[®] films after exposure to aerosols in the lung relevant surface pressure range. Particle deposition was performed during the first expansion cycle. Surfactant films were compressed and expanded at a speed of 150 mm/min with a surface area change of about 25 cm² (between surface areas of 210 cm² and 185 cm² for DPPC, and 198 cm² and 124 cm² for Infasurf[®] films). Error bars represent the standard deviation.

surfactant function under breathing conditions. The surface pressure versus surface area isotherms for pure DPPC monolayers during the second, fifth, and tenth compression and expansion cycles in the lung relevant range are presented in Figure 7a and the maximum surface pressure at the end of each compression cycle are shown in Table 1 (second column).

The maximum surface pressure values decreased as the surface area cycling proceeded due to the ejection of DPPC molecules from the air–water interface at the end of each compression cycle. This is the same phenomenon previously reported for DPPC molecules compressed to high surface pressure values.^(4,11) Aerosol application was then performed on DPPC monolayers with a single exposure during surface expansion in the first cycle. Particles were introduced to the surfactant surface during area expansion since this better mimics lung exposure during inhalation. This also allowed the surface pressure at the end of the first compression cycle before exposure to the particles to be used as an internal control to ensure that differences in the surface pressure isotherms were caused solely by the deposited particles. The maximum surface pressure at the end of the first compression cycle were similar in all experiments, confirming the reproducibility of isotherms before exposure to particles (Table 1, first row of the second and third

TABLE 1. PARTICLE EFFECTS ON THE MAXIMUM SURFACE PRESSURE OBTAINED UPON COMPRESSION OF DPPC AND INFASURF[®] FILMS DURING SURFACE AREA CYCLING IN THE LUNG RELEVANT SURFACE PRESSURE RANGE

Cycle	Maximum Surface Pressure (mN/m)			
	Pure DPPC	DPPC exposed to particles	Pure Infasurf [®]	Infasurf [®] exposed to particles
1 st	71.0 ± 1.7	70.2 ± 1.2	66.6 ± 0.3	66.2 ± 1.0
2 nd	70.2 ± 1.3	51.0 ± 2.8	66.3 ± 0.4	60.0 ± 3.4
3 rd	69.2 ± 1.7	51.8 ± 2.0	65.3 ± 0.6	58.6 ± 2.9
4 th	67.9 ± 1.9	52.0 ± 2.0	62.6 ± 1.8	55.2 ± 3.5
5 th	66.4 ± 2.0	52.0 ± 2.1	60.2 ± 2.1	52.8 ± 4.7
6 th	65.1 ± 1.9	52.1 ± 2.1	57.2 ± 3.3	51.3 ± 4.4
7 th	64.8 ± 2.4	51.6 ± 2.2	54.8 ± 3.4	49.3 ± 3.2
8 th	63.9 ± 2.3	51.4 ± 2.4	52.1 ± 3.1	48.1 ± 2.4
9 th	63.0 ± 2.3	51.2 ± 2.3	50.5 ± 2.5	46.8 ± 1.7
10 th	62.1 ± 2.2	52.2 ± 2.4	48.9 ± 2.0	46.1 ± 1.6

Carboxyl modified polystyrene particles were delivered at a dose of 0.058 ± 0.004 g/m² for DPPC and 0.045 ± 0.004 g/m² for Infasurf[®].

column). Exposure to particles resulted in a significant reduction in the maximum surface pressure during cycling (Fig. 7b and Table 1). Although particle deposition was performed only once in the first cycle, the surface pressure reduction persisted through all cycles. The maximum surface pressure at the end of the last cycle was significantly different after particle deposition compared to pure DPPC films (52.2 ± 2.4 mN/m vs. 62.1 ± 2.2 mN/m).

Surface pressure vs. surface area isotherms for Infasurf[®] films during sequential compression and expansion in the lung relevant surface pressure range are shown in Figure 7c. Similar to DPPC, a reduction in the maximum surface pressure values upon cycling was observed from the first to the tenth cycle due to ejection of surfactant molecules to the subphase at the end of each cycle (Table 1, fourth column). Previously published results on compression–expansion cycling of Infasurf[®] have shown a similar reduction in the maximum surface pressure at fixed surface areas.⁽³⁸⁾ Particle deposition on the Infasurf[®] films induced changes in the maximum surface pressure (Fig. 7d). The presence of particles resulted in a significant reduction in the maximum surface pressure values of the second to the fifth cycle, but not the following cycles (Table 1, fourth and fifth columns). In addition, the difference in the maximum surface pressure of Infasurf[®] films was not as pronounced as that observed with DPPC monolayers. For example, at the end of the second cycle, an increase in the maximum surface pressure of 6.2 mN/m was observed for Infasurf films exposed to particles compared to an increase of 19.2 mN/m for DPPC monolayers. Interestingly, the maximum surface pressure of Infasurf[®] films with and without particles was not significantly different from the sixth to the tenth cycle, suggesting that particle effects do not persist in destabilizing the interfacial properties of Infasurf[®].

Discussion

Interactions between particles and lung surfactant films have received attention in recent years as our knowledge of the negative health impacts of aerosols has expanded.⁽³⁹⁾ One factor that may contribute to deterioration of lung health upon particle exposure is disruptions to lung surfactant function. While our ability to monitor lung surfactant function *in vivo* directly is limited, there is considerable precedence for studying surfactant function *in vitro*. In particular, *in vitro* studies have been invaluable in elucidating the mechanisms of surfactant-induced lung disease. For example, the role of the pulmonary surfactant in neonatal respiratory distress was uncovered for the first time using *in vitro* studies.⁽⁴⁰⁾ Similarly, *in vitro* studies have exposed the mechanisms of surfactant inhibition by serum proteins, thereby revealing the likely mechanisms of surfactant dysfunction in adult respiratory distress syndrome.⁽⁴¹⁾

With increased awareness of human exposure to small particles of environmental and medical origin, studies of particle–surfactant interactions have gained attention as they allow prediction of potential particle-induced disruptions to surfactant function. While several studies have reported surfactant inhibition *in vitro* due to particle exposure, these studies have utilized systems that are not representative of a realistic inhalation exposure. The effects of particles on the interfacial properties of surfactants have been investigated by various techniques, including the Langmuir–Wilhelmy balance, pul-

sating bubble surfactometer, and captive bubble tensiometer. However, in these prior studies, particles have been either suspended beneath the surfactant film,^(4–6,10–12,16–18,20,42) incubated with surfactant before spreading the surfactant film,^(8,21) or mixed with surfactant at the time of measurement,^(7,20) none of which represent exposure to aerosols. While the need for techniques that enable the study of aerosols on surfactant function has been noted,⁽²⁰⁾ this has not been achieved to date and thus these interactions remain poorly understood. In the current study, a method to apply aerosols on surfactant films was developed, thereby enabling a better understanding of aerosol particle-induced surfactant dysfunction.

Dry particles were suspended in air using a Dry Powder Insufflator[™] maintained at a distance away from the surface to limit interfacial disturbances (Fig. 1). Polystyrene particles were used as a model particle system for these studies due to their stability in solution, which enables a better understanding of the specific effects due to particles rather than degradation products or leached agents, and their similarity in physical and chemical properties to other commonly used polymeric particles being tested as inhaled drug delivery systems. A particle size of 200 nm was used in these studies, as smaller particles have often been shown to elicit larger effects on surfactant function and this particle size is of relevance to drug delivery.⁽⁴³⁾ Although more than half of the particles remained as singlets following deposition on the surface, agglomerates with a diameter of up to 10 μ m were also observed under electron microscopy (Fig. 2).

According to the classical Darjeuin, Landau, Verwey and Overbeek (DLVO) theory, interparticle forces are described by the interplay between attractive van der Waals forces promoting particle aggregation and electrostatic repulsive forces promoting particle stability.⁽⁴⁴⁾ The agglomeration of dry particles in this study is due to the lower permittivity of air compared to aqueous media, which reduces the electrostatic repulsive forces between the particles leading to aggregation. Both nanoparticles and agglomerates of nanoparticles deposit in the alveolar region of the lungs with reasonable efficiency, although particle interactions with cells is different based on particle size.⁽⁴⁵⁾ An estimated 20% of inhaled particles with a diameter of 200–500 nm have been predicted to deposit in the alveoli, with the remainder being exhaled. However, a higher fraction (upwards of 90%) of particles with larger diameters in the 1–5 micron range achieve alveolar deposition. Thus, these particles would be expected to deposit in the alveolar region as both single particles with about 20% efficiency, as well as particle agglomerates with higher efficiency. In this study, particle deposition onto the surfactant surface was reproducible with 60%–70% of the generated aerosols depositing on the surfactant surface and standard deviations within 15% of the mean. Deposition was not significantly affected by changing the trough surface area. Light absorbance has been used to measure the size of a wide range of particle diameters (100 nm to 1000 nm), though it is limited to measurements with fairly monodisperse particles.⁽³¹⁾

Dry particles that deposited onto the DPPC films altered the interfacial properties of the film when the surface area was reduced (Fig. 4). The surface area at which the monolayer collapsed was reduced in the presence of particles (162 ± 3 cm² with particles vs. 174 ± 3 cm² for pure DPPC films), but the surface pressure at which collapse occurred

was not affected (maintained at 72 mN/m). This suggests that a small quantity of surfactant molecules were lost from the surface upon particle deposition, likely due to adsorption onto the particle surfaces. It has been previously reported that DPPC is the major component adsorbed onto urban fine particles (PM_{2.5}) when the particles were exposed to bronchoalveolar lavage (BAL) fluid.⁽⁴⁶⁾ Thus, it is expected that a similar adsorption phenomenon occurred in the present study, thereby reducing the amount of DPPC at the air–water interface. Other studies have shown that when particles or drug compounds remain at the surfactant interface, high surface pressures cannot be reached upon compression.^(47,48) Thus, the observation that the collapse surface pressure remained at 72 mN/m suggests that at the time of collapse no particles remained at the air–water interface at the time of collapse. This is in line with studies conducted by Schurch et al.⁽⁴⁹⁾ and Gehr et al.,⁽⁵⁰⁾ who observed complete particle submersion beneath surfactant films at low surface tensions (high surface pressures).

When deposited onto the more complex Infasurf[®] films, particles altered both the collapse surface area and surface pressure (Fig. 4). While the change in the collapse surface area was only slightly higher than that observed for DPPC films ($129 \pm 2 \text{ cm}^2$ with particles vs. $149 \pm 4 \text{ cm}^2$ for pure Infasurf[®] films), the change in the collapse surface pressure was only observed for the Infasurf films. This change in surface pressure suggests that surfactant components required to achieve high surface pressure were adsorbed onto particle surfaces. Infasurf[®] contains surfactant proteins B and C, which are positively charged and are likely to be adsorbed on the surface of negatively charged particles.⁽⁵¹⁾ In fact, adsorption of Infasurf[®] proteins by negatively charged particles has been reported previously.¹⁰ Alternatively, we have previously observed the adsorption of lipid molecules, DPPC, onto polystyrene particles.⁽³²⁾

Studies of particle effects on surfactant function at longer interaction times are physiologically important as the time required for a complete turnover of lung surfactant molecules is approximately 11 hours.⁽⁵²⁾ Although surfactant is constantly being produced by Type II alveolar cells, production may not occur as quickly as surfactant is removed by particles via adsorption. Furthermore, it has been shown that particle attachment to alveolar macrophages is dependent on particle size and submicron particles show less association with macrophages after 4 hours of incubation.⁽²²⁾ Thus, studies of particle–surfactant interactions after 3 to 6 hours have physiological significance. In the current study, longer interaction times generated a larger detrimental effect on surfactant function (Fig. 6). The collapse point was shifted to smaller surface areas suggesting that more surfactant molecules were removed from the surface, requiring a large surface area change to induce collapse. The dependence of these particle-induced effects on time suggests a time-dependent adsorption of surfactant components on particle surfaces. Fan and colleagues⁽¹⁰⁾ reported a similar but more pronounced effect than observed in the current study following increased interaction time between Infasurf[®] films and hydroxyapatite particles. This is likely due to the higher concentration of particles used by Fan et al. compared to the present study (0.05 g/L vs. $\sim 0.01 \text{ g/L}$ in the current study), in addition to the smaller size and thus larger surface area of the hydroxyapatite particles used in that study (hydrodynamic diameter of 93 nm).

Interestingly, deposition of particles during compression of the Infasurf[®] film (at surface pressures of 25 mN/m and 43 mN/m) rather than prior to compression (at surface pressure close to 0 mN/m) led to the disappearance of the effects observed on surfactant collapse surface pressure and surface area (Fig. 5). This observation suggests that, when particles are deposited as aerosols on the surfactant surface, their interaction with surfactant is dependent on the structure of the surfactant film. This is of significant importance for considerations of particle–surfactant interactions. The surface pressure of native lung surfactant is reported to always be above 30 mN/m, even during inhalation,^(26–28) suggesting that deposition of aerosols on a compressed surfactant film (i.e., at higher surface pressures) better represents particle interactions in the lungs. It further suggests that *in vitro* particle–surfactant interaction studies reported in the literature to date may not be relevant to aerosol exposures, as these studies have been performed at an initial surface pressure close to zero.

We chose to take these studies one step further to better mimic particle–surfactant interactions during respiration by inducing fast surfactant cycling in the lung-relevant surface pressure range. We estimated the surface area range over which the trough system would match changes to surface area in the lungs via *in vivo* surface pressure measurements (see Section Surface Pressure vs. Surface Area Isotherms for more details). Dry particles were suspended in air and deposited onto the films during the first expansion, which would correspond to an inhalation *in vivo*. Then ten consecutive cycles of compression and expansion were performed. The fast rate of surface area modification (150 mm/min, the highest rate available on the Langmuir trough instrument) led to a cycle time of 20 sec for DPPC and 43 sec for Infasurf[®]. While this cycling rate is still about 5 to 10 times lower than the rate of lung surface area cycling during normal breathing (assuming a resting breathing rate of 15 breaths/minute),³⁰ these studies allowed us to evaluate the effect of cycling rate on surfactant function and particle–surfactant interactions.

DPPC isotherms generated during fast surface area cycling in the lung relevant surface pressure range exhibited a small reduction in surface pressure upon cycling, which is in agreement with the study by Hildebran et al.⁽⁵³⁾ (Fig. 7a). The deposition of dry particles onto the DPPC films during the first expansion cycle caused a pronounced drop in the maximum surface pressure achieved (Fig. 7b and Table 1). This drop was significantly larger than the reduction of surface pressure observed in the monolayer collapse studies (19 mN/m in fast cycling vs. 4 mN/m in collapse studies) and persisted even after 10 cycles. In contrast, Infasurf[®] films exhibited a less pronounced drop in maximum surface pressure that did not persist beyond the fifth cycle (Fig. 7c and 7d), suggesting an ability of Infasurf[®] to compensate for a small loss in surfactant molecules. While re-adsorption of ejected DPPC molecules to the air–water interface is slow, in Infasurf this process is facilitated by hydrophobic surfactant proteins giving the surfactant the ability to recover when surface area becomes available for ejected surfactant (i.e., during surface expansion).⁽⁵⁴⁾ This result is in accordance with the study of Tatur and Badia who observed that gold nanoparticles affect the microstructure of DPPC films but not Survanta, another complex surfactant used clinically.⁽⁵⁵⁾

It is important to note that particle effects on surfactant function during fast cycling studies in the lung relevant

surface pressure were different compared to monolayer collapse studies. We theorize that these changes are due to the re-expansion of the surface in the cycling studies, which provides free space for collapsed surfactant components to re-adsorb to the interface and thus compensate for the inhibitory effects of particles. Since the submerged molecules re-adsorb to the surface much faster in the case of Infasurf[®] than in the case of DPPC, the dip in surface pressure persists for DPPC throughout the cycles (because fast cycling is not giving the molecules time to come back), but not Infasurf[®]. It should be mentioned that the low surface tension of surfactants will likely result in particle ejection from the interface at the time of contact. Ejected particles are unlikely to re-adsorb at the air–water interface due to the low surface tension at the fluid surface, even during the expansion cycle and the expected hydrophilicity of the particles due to protein adsorption to the particle surface.

Due to compact surfactant structure, faster rate of surface area alteration, and the possibility to study surfactant function after rapid surface area expansions, lung relevant studies provide information that cannot be obtained in traditional monolayer collapse studies. Also, in the collapse studies the particles are expected to remain at the air–water interface upon deposition due to the high starting surface tension values (~ 72 mN/m). However, in the lung relevant studies, particles deposit on a lower surface tension fluid and thus are more likely to immediately submerge. This better mimics observations made *in vivo* of particle submersion within lung fluids.^(49,55) Overall, the effects observed with lung relevant studies are different compared to monolayer collapse studies and are a better representative of particle–surfactant interactions. Thus, we believe that monolayer collapse studies should be used to supplement information obtained by cycling studies in the lung relevant surface pressure range to enhance our understanding of the mechanisms by which particles induce surfactant dysfunction.

While these studies provide a method to expose surfactant films to aerosols more realistically, a few limitations in these studies exist. Deposition of aerosols is an important aspect of particle–surfactant interactions, though a more realistic system can be obtained by also using physiologically relevant temperature and humidity. The near saturation humidity levels in the lungs may lead to hygroscopic growth of particles and thereby affect particle–surfactant interactions. Also, the observations of the current study are valid for polymeric particles with highly negative surface charge and should not be generalized to particles of different physicochemical properties. Particle charge might play a big role in particle–surfactant interactions (e.g., specific adsorption of certain surfactant components). For future studies, the aerosol deposition system developed here can be used with particles of various physicochemical properties to elucidate the mechanisms of surfactant–particle interaction.

Conclusions

In the current study, we developed a method to study particle–lung surfactant interactions in a manner closer to the *in vivo* situation (i.e., suspension of the particles in air and deposition of the resulting aerosol onto the surfactant surface), as well as performance of surface area cycling under conditions that reach speeds close to those during

normal breathing and within a narrow surface area range. The observation that Infasurf was able to restore its function quickly after exposure to aerosols under these conditions suggests that particle-induced surfactant inhibition is unlikely to occur *in vivo* due to an aerosol exposure. Future studies are needed to examine whether more toxic particles, such as environmentally-derived particles, exhibit an inhibitory effect on lung surfactant function under more physiologically-relevant conditions.

Acknowledgments

The authors gratefully acknowledge ONY Inc. for donation of Infasurf[®]. Financial support was provided by the University of Iowa's Center for Health Effects of Environmental Contamination, the Environmental Health Sciences Research Center (NIH P30 ES005605), and the Executive Council for Graduate and Professional Students (AF). The authors thank Dr. Vicki Grassian for the use of the surface area analyzer, and University of Iowa's Central Microscopy Research Facility and the Office for the Vice President of Research for access to the electron microscopes and XPS. Dr. Jonas Baltrusaitis is acknowledged for performing the XPS experiments.

Author Disclosure Statement

No conflicts of financial interest exist.

References

1. Frerking I, Gunther A, Seeger W, and Pison U: Pulmonary surfactant: Functions, abnormalities and therapeutic options. *J Intensive Care Med.* 2001;27:1699–1717.
2. Al-Hallak MHDK, Azarmi S, Sun C, Lai P, Prenner EJ, Roa W, and Lobenberg R: Pulmonary toxicity of polysorbate-80-coated inhalable nanoparticles *in vitro* and *in vivo* evaluation. *AAPS J.* 2010;12:294–299.
3. Bakshi MS, Zhao L, Smith R, Possmayer F, and Petersen NO: Metal nanoparticle pollutants interfere with pulmonary surfactant function *in vitro*. *Biophys J.* 2008;94:855–868.
4. Guzman E, Liggieri L, Santini E, Ferrari M, and Ravera F: DPPC-DOPC Langmuir monolayers modified by hydrophilic silica nanoparticles: Phase behaviour, structure and rheology. *Colloids Surf A, Physicochem Eng Asp.* 2011; 174–183.
5. Guzman E, Liggieri L, Santini E, Ferrari M, and Ravera F: Effect of hydrophilic and hydrophobic nanoparticles on the surface pressure response of DPPC monolayers. *J Phys Chem C, Nanomater Interfaces.* 2011;115:21715–21722.
6. Guzman E, Liggieri L, Santini E, Ferrari M, and Ravera F: Mixed DPPC–cholesterol Langmuir monolayers in presence of hydrophilic silica nanoparticles. *Colloids Surf B, Biointerfaces.* 2013;105:284–293.
7. Schleh C, Muhlfield C, Pulskamp K, Schmiedel A, Nassimi M, Lauenstein HD, Braun A, Krug N, Erpenbeck VJ, and Hohlfeld JM: The effect of titanium dioxide nanoparticles on pulmonary surfactant function and ultrastructure. *Respir Res.* 2009;10:90–101.
8. Beck Broichsitter M, Ruppert C, Schmehl T, Guenther A, Betz T, Bakowsky U, Seeger W, Kissel T, and Gessler T: Biophysical investigation of pulmonary surfactant surface properties upon contact with polymeric nanoparticles *in vitro*. *Nanomedicine.* 2010;7:341–350.

9. Dwivedi MV, Harishchandra RK, Koshkina O, Maskos M, and Galla HJ: Size influences the effect of hydrophobic nanoparticles on lung surfactant model systems. *Biophys J*. 2014;106:289–298.
10. Fan Q, Wang YE, Zhao X, Loo JSC, and Zuo YY: Adverse biophysical effects of hydroxyapatite nanoparticles on natural pulmonary surfactant. *ACS Nano*. 2011;5:6410–6416.
11. Farnoud AM, and Fiegel J: Low concentrations of negatively charged sub-micron particles alter the microstructure of DPPC at the air-water interface. *Colloids Surf A, Physicochem Eng Asp*. 2012;415:320–327.
12. Farnoud AM, and Fiegel J: Interaction of dipalmitoyl phosphatidylcholine monolayers with a particle-laden sub-phase. *J Phys Chem B*. 2013;117:12124–12134.
13. Valle RP, Huang CL, Loo SCJ, and Zuo YY: Increasing hydrophobicity of nanoparticles intensifies lung surfactant film inhibition and particle retention. *ACS Sustainable Chem Eng*. 2014;2:1574–1580.
14. Im Hof V, Gehr P, Gerber V, Lee M, and Schurch S: *In vivo* determination of surface tension in the horse trachea and in vitro model studies. *Respir Physiol Neurobiol*. 1997;109:81–93.
15. Duncan SL, and Larson RG: Comparing experimental and simulated pressure-area isotherms for DPPC. *Biophys J*. 2008;94:2965–2986.
16. Harishchandra RK, Saleem M, and Galla HJ: Nanoparticle interaction with model lung surfactant monolayers. *J R Soc Interface*. 2010;7:15–26.
17. Kanishtha T, Banerjee R, and Venkataraman C: Effect of particle emissions from biofuel combustion on surface activity of model and therapeutic pulmonary surfactants. *Environ Toxicol Pharmacol*. 2006;22:325–333.
18. Lai P, Nathoo S, Ku T, Gill S, Azarmi S, Roa W, Lobenberg R, and Prenner EJ: Real-time imaging of interactions between dipalmitoylphosphatidylcholine monolayers and gelatin based nanoparticles using Brewster angle microscopy. *J Biomed Nanotechnol*. 2010;6:145–152.
19. Sosnowski TR, Gradon L, and Podgorski A: Influence of insoluble aerosol deposits on the surface activity of the pulmonary surfactant: A possible mechanism of alveolar clearance retardation? *Aerosol Sci Tech*. 2000;32:52–60.
20. Stuart D, Lobenberg R, Ku T, Azarmi S, Ely L, Roa W, and Prenner EJ: Biophysical investigation of nanoparticle interactions with lung surfactant model systems. *J Biomed Nanotechnol*. 2006;2:245–252.
21. Beck-Broichsitter M, Ruppert C, Schmehl T, Gunther A, and Seeger W: Biophysical inhibition of synthetic vs. naturally-derived pulmonary surfactant preparations by polymeric nanoparticles. *Biochim Biophys Acta*. 2014;1838:474–481.
22. Doshi N, and Mitragotri S: Macrophages recognize size and shape of their targets. *PLoS One*. 2010;5:e10051.
23. Champion JA, Walker A, and Mitragotri S: Role of particle size in phagocytosis of polymeric microspheres. *Pharmaceut Res*. 2008;25:1815–1821.
24. Abramoff MD, Magalhaes PJ, and Ram SJ: Image processing with ImageJ. *Biophotonics Intl*. 2004;11:36–42.
25. Hardy NJ, Richardson TH, and Grunfeld F: Minimising monolayer collapse on Langmuir troughs. *Colloids Surf A Physicochem Eng Asp*. 2006;284–285:202–206.
26. Bachofen H, Schurch S, Urbinelli M, and Weibel E: Relations among alveolar surface tension, surface area, volume, and recoil pressure. *J Appl Physiol*. 1987;62:1878–1887.
27. Horie T, Ardila R, and Hildebrandt J: Static and dynamic properties of excised cat lung in relation to temperature. *J Appl Physiol*. 1974;36:317–322.
28. Schurch S, Bachofen H, and Weibel ER: Alveolar surface tensions in excised rabbit lungs: Effect of temperature. *Respir Physiol Neurobiol*. 1985;62:31–45.
29. Smith JC, and Stamenovic D: Surface forces in lungs. I. Alveolar surface tension-lung volume relationships. *J Appl Physiol*. 1986;60:1341–1350.
30. Levitzky MG: *Pulmonary Physiology: Lange Physiology Series*. McGraw-Hill: New York City, NY: 1995; p. 57.
31. Irache J, Durrer C, Ponchel G, and Duchene D: Determination of particle concentration in latexes by turbidimetry. *Int J Pharm*. 1993;90:9–12.
32. Farnoud AM: Interaction of polymeric particles with surfactant interfaces. PhD Thesis. The University of Iowa, 2013.
33. Lee KYC: Collapse mechanisms of Langmuir monolayers. *Annu Rev Phys Chem*. 2008;59:771–791.
34. Wustneck R: Interfacial properties of pulmonary surfactant layers. *Adv Colloid Interface Sci*. 2005;117:33–58.
35. Bloom BT, Kattwinkel J, Hall RT, Delmore PM, Egan EA, Trout JR, Malloy MH, Brown DR, Holzman IR, and Coghill CH: Comparison of Infasurf (calf lung surfactant extract) to Survanta (Beractant) in the treatment and prevention of respiratory distress syndrome. *Pediatrics*. 1997;100:31–38.
36. Wang YE, Zhang H, Fan Q, Neal CR, and Zuo YY: Biophysical interaction between corticosteroids and natural surfactant preparation: Implications for pulmonary drug delivery using surfactant as a carrier. *Soft Matter*. 2012;8:504–511.
37. Zhang H, Fan Q, Wang YE, Neal CR, and Zuo YY: Comparative study of clinical pulmonary surfactants using atomic force microscopy. *Biochim Biophys Acta*. 2011;1808:1832–1842.
38. Zhang H, Wang YE, Fan Q, and Zuo YY: On the low surface tension of lung surfactant. *Langmuir*. 2011;27:8351–8358.
39. Kendall M, and Holgate S: Health impact and toxicological effects of nanomaterials in the lung. *Respirology*. 17:743–758.
40. Avery ME, and Mead J: Surface properties in relation to atelectasis and hyaline membrane disease. *Arch Pediatr Adolesc Med*. 1959;97:517–523.
41. Holm BA, Notter R, and Finkelstein JN: Surface property changes from interactions of albumin with natural lung surfactant and extracted lung lipids. *Chem Phys Lipids*. 1985;38:287–298.
42. Ku T, Gill S, Lobenberg R, Azarmi S, Roa W, and Prenner EJ: Size dependent interactions of nanoparticles with lung surfactant model systems and the significant impact on surface potential. *J Nanosci Nanotechnol*. 2008;8:2971–2978.
43. Trivedi R, Redente EF, Thakur A, Riches DW, and Kompella UB: Local delivery of biodegradable pirfenidone nanoparticles ameliorates bleomycin-induced pulmonary fibrosis in mice. *Nanotechnology*. 2012;23:505101.
44. Berg JC: *Introduction to Interfaces and Colloids*. World Scientific: Hackensack, NJ; 2009; pp. 547–550.
45. Lippmann M: Regional deposition of particles in the human respiratory tract. In: DHK Lee, HL Falk, SD Murphy, (eds). *Handbook of Physiology, Section 9: Reactions to Environmental Agents Handbook of Physiology, Section 9: Reactions to Environmental Agents*, American Physiology Society, Bethesda, MD; 1977; pp. 213–232.
46. Kendall M: Fine airborne urban particles (PM 2.5) sequester lung surfactant and amino acids from human lung

- lavage. *Am J Physiol Lung Cell Mol Physiol.* 2007;293:1053–1058.
47. Wang Z, Li X, and Yang S: Studies of dipalmitoylphosphatidylcholine (DPPC) monolayers embedded with endohedral metallofullerene (Dy@ C82). *Langmuir.* 2009;25:12968–12973.
48. Wiecek A, Dyranowicz-Latka P, Vila-Romeu N, Nieto-Suarez M, and Flasiński M: Interactions between an anticancer drug—edelfosine—and DPPC in Langmuir monolayers. *Colloids Surf A, Physicochem Eng Asp.* 2008;321:201–205.
49. Schurch S, Gehr P, Im Hof V, Geiser M, and Green F: Surfactant displaces particles toward the epithelium in airways and alveoli. *Respir Physiol Neurobiol.* 1990;80:17–32.
50. Gehr P, Geiser M, Im Hof V, Schurch S, Waber U, and Baumann M: Surfactant and inhaled particles in the conducting airways: Structural, stereological, and biophysical aspects. *Microsc Res Tech.* 1993;26:423–436.
51. Perez Gil J: Interfacial properties of surfactant proteins. *Biochim Biophys Acta.* 1998;1408:203.
52. Baritussio AG, Magoon MW, Goerke J, and Clements JA: Precursor-product relationship between rabbit type II cell lamellar bodies and alveolar surface-active material: surfactant turnover time. *Biochim Biophys Acta.* 1981;666:382–393.
53. Hildebran JN, Goerke J, and Clements JA: Pulmonary surface film stability and composition. *J Appl Physiol Respir Environ Exerc Physiol.* 1979;47:604–611.
54. Possmayer F, Nag K, Rodriguez K, Qanbar R, and Schurch S: Surface activity *in vitro*: Role of surfactant proteins. *Comp Biochem Physiol A Mol Integr Physiol.* 2001;129:209–220.
55. Tatur S, and Badia A: Influence of hydrophobic alkylated gold nanoparticles on the phase behavior of monolayers of DPPC and clinical lung surfactant. *Langmuir.* 2012;28:628–639.
56. Geiser M, Schurch S, and Gehr P: Influence of surface chemistry and topography of particles on their immersion into the lung's surface-lining layer. *J Appl Physiol.* 2003;94:1793–1801.

Received on July 12, 2014
in final form, November 28, 2014

Reviewed by:
Marianne Geiser
Robert Tilton

Address correspondence to:
Jennifer Fiegel, PhD
Department of Pharmaceutical Sciences
and Experimental Therapeutics
The University of Iowa
115 South Grand Ave., S215 Pharmacy Building
Iowa City, IA 52242

E-mail: jennifer-fiegel@uiowa.edu